



Geochemistry of Mafic-Intermediate Intrusive Rocks from the Twangiza-Namoya Gold Belt, Eastern Democratic Republic of Congo: Trace Element Constraints on their Origin, Petrogenesis and Tectonic Setting

Gerald L. Chuwa* and Charles H. Kasanzu

Department of Geosciences, University of Dar es Salaam, P.O. Box 35052, Dar es Salaam, Tanzania.

E-mail addresses: gerald7chuwa@gmail.com; kcharls16@yahoo.com

*Corresponding author

Received 10 Aug 2021, Revised 10 Mar 2022, Accepted 19 Mar 2022, Published Mar 2022

DOI: <https://dx.doi.org/10.4314/tjs.v48i1.7>

Abstract

Bulk geochemical data for the Twangiza-Namoya Gold Belt, Democratic Republic of Congo, are presented in order to classify the rock assemblages, elucidate their petrogenesis and tectonic settings. Nb/Yb and Zr/Ti constraints reveal two suites for the rocks: sub-alkaline to andesitic basalts (Suite-1); and alkaline basalts (Suite-2). Ratios of Ti/Zr = 22–70; Zr/Hf = 35–42; Nb/Ta = 12–13; Nb/Th = 1–2 and La/Nb = 2.4–3.8 suggest arc-generated mantle melts with crustal inputs and arc-fluids metasomatism for Suite-1. The samples have positive LILE and negative Nb, Ta, Ti anomalies, enrichments in the LREE over middle and HREE ($(La/Yb)_{CN} = 3.6–8.9$ with negative Eu anomalies (0.7–0.9) in Chondrite-normalized diagrams. Yb-Th/Ta and Ta/Yb-Th/Yb ratios suggest active continental margin settings, whereas Ta/Hf-Th/Ta and Nb/Yb-Th/Yb diagrams suggest a depleted MORB source. Ti/Zr, Zr/Hf, Nb/Ta, Nb/Th and La/Nb constraints for Suite-2 suggest MORB and oceanic plateau basaltic sources. REE patterns show enrichments in the LREE with negative to positive Eu anomalies (0.7–1.3). Yb-Th/Ta and Ta/Yb-Th/Yb ratios suggest a within plate tectonic setting. It is suggested that Suite-2 rocks were sourced from mantle-derived melts with a composition between an enriched MORB to OIB.

Keywords: Twangiza-Namoya; Petrogenesis; Tectonic setting; Trace element ratios.

Introduction

Multiple episodes of magmatism and orogenic activities during the Mesoproterozoic and Neoproterozoic periods characterise the tectonic evolution of the Karagwe-Ankolean Belt (KAB) in Central Africa (Tack et al. 2010, Fernandez-Alonso et al. 2012). The Twangiza-Namoya Gold Belt (TNGB) in the Democratic Republic of Congo (DRC) is located in the western part of the KAB (Figures 1 and 2). The belt comprises metasedimentary rocks that are intruded by mafic-ultramafic, intermediate and felsic rocks dated between ~ 1400 Ma and 900 Ma (Walemba and Master 2005,

Fernandez-Alonso et al. 2012). Geochemical characteristics of such magmatic rocks can assist in constraining petrogenesis and paleotectonic settings during the Precambrian (Best 2002).

Extensive investigations carried out in the eastern part of the KAB (in Rwanda and Burundi) applied a combination of geochemical, geophysical and geochronological techniques (e.g. Klerkx et al. 1987, Koegelenberg and Kisters 2014). Conversely, the western part (mainly in the eastern DRC) has not received similar research interests due to poor accessibility. As a result, the TNGB geological settings,

geochemical characteristics and geochronology are poorly understood. The purpose of this study, therefore, is to constrain the origin, petrogenesis and infer tectonic settings of the mafic-intermediate igneous rocks in the region.

Geological Setting

Regional geology

TNGB lies in the Mesoproterozoic orogenic belt of central Africa (Hanson 2003) that is made up of the northern KAB and the southern Kibaran Belt (KIB, Figure 1). The NW-SE oriented Paleoproterozoic Ubendian-Rusizian Belt in eastern DRC separates the two belts (Fernandez-Alonso et al. 2012, Figure 1). The KAB comprises the Kagera and the Akanyaru Supergroups in the east and west, respectively, that correspond to the eastern domain (ED) and western domain

(WD) as reported in Tack et al. (2010) and Fernandez-Alonso et al. (2012, Figure 1). The Akanyaru Supergroup comprises metasedimentary rocks that overlie the Ubendian-Rusizian rocks. Stratigraphically, the Akanyaru Supergroup underlies the Neoproterozoic Itombwe Supergroup molasse sequences (Walemba and Master 2005). Two contrasting tectonic models attempt to explain the KAB geodynamic setting and evolution. The first model interprets the KAB to have developed in the Mesoproterozoic extension-compressional settings of the proto-Congo craton that existed as a coherent entity since 1375 Ma (Tack et al. 2010, Fernandez-Alonso et al. 2012). The second model favours the Mesoproterozoic subduction-collisional setting in the KAB (Koegelenberg and Kisters 2014, Debruyne et al. 2015).

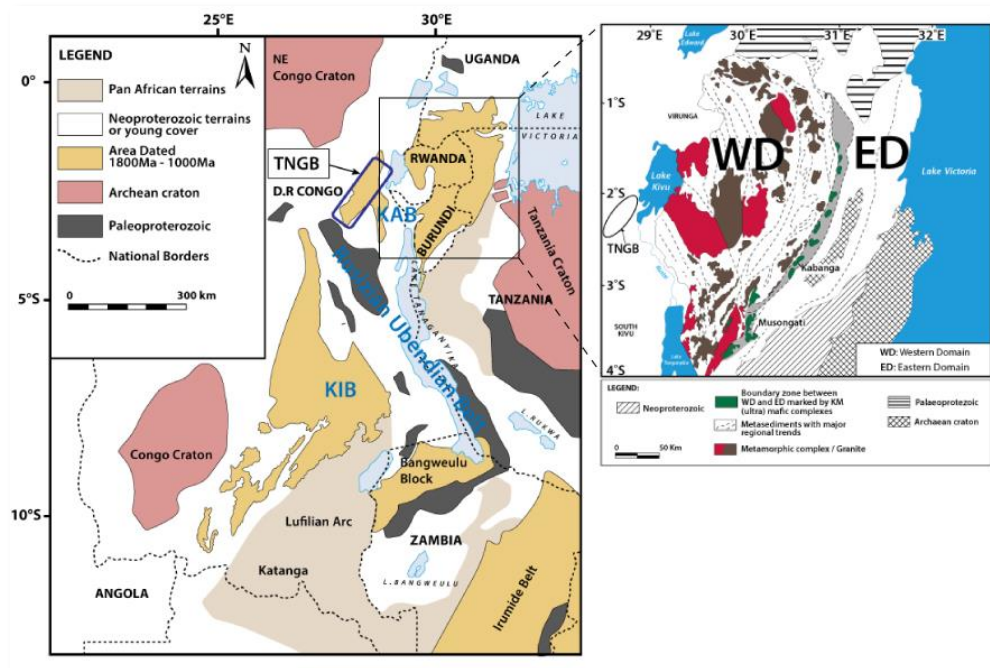


Figure 1: Regional geological framework of the Central Africa region. The insert map refers to the Kabanga-Musongati mafic ultramafic intrusions alignment (Map from Fernandez-Alonso et al. 2012).

Local geology

The study area is underlain by N-S trending rock sequences that extend for over 7 km (Walemba 2001). The rocks comprise mudstones, shales, phyllites, siltstone, sandstone and diamictites that are weakly metamorphosed into greenschist facies (Walemba and Master 2005). The sequences are intruded by several mafic sills that are referred to as feldspar porphyries and gabbros (Pohl et al. 2013). The Lugushwa and Kamituga sites comprise metapelite, graphitic metapelite, shale, metasiltstone, schist and

quartzite. These rocks strike NE-SW and dip towards the south-east. Post deformation pegmatite dykes are also common and are associated with the Neoproterozoic granitic intrusions.

Namoya geology comprises strongly foliated sericite-chlorite and graphitic-schist interbedded with quartz-mica schist whose foliations strike NW-SE, dipping N-E. These rocks are intruded by multiple sills of dolerite, quartz-diorite and feldspar porphyry up to 80 m thick.

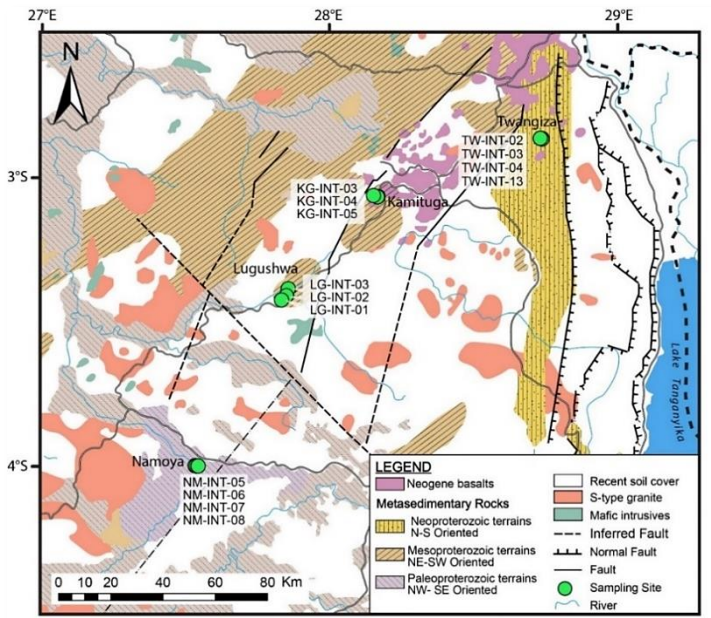


Figure 2: A map showing the local geology of the studied area and location of the samples (modified from Milesi et al. 2006).

Materials and Methods

The study used petrography and whole-rock geochemistry of 13 samples collected from 4 localities, namely Twangiza, Namoya, Lugushwa and Kamituga (Figure 2). For geochemical analysis, a 0.25 g sample was mixed with a flux of lithium metaborate and lithium tetraborate for induction furnace. The resulting melt was immediately poured into a solution of 5% HNO₃ containing an internal standard, thoroughly mixed for approximately 30 minutes to achieve complete dissolution. The sample solution

aliquots were analysed for major elements and trace element Sc, on a combination of Thermo Jarrell-Ash ENVIRO II ICP-OES using major elements detection limits of 0.01 wt.% and Sc detection limit 2 ppm (Olesik 1991). Loss on ignition was determined from the weight loss after heating the samples at 1050 °C for 2 hours.

Another aliquot of the original sample was spiked with internal In and Rh standards to cover a broad mass range and diluted by a factor of 6000 times before being introduced into a Perkin Elmer Sciex Elan 6000 ICP-MS

for trace element analysis (Olesik 1991, Jenner 1996). Trace elements analytical reproducibility is better than 10% for most elements. Trace elements analytical reproducibility for replicate analyses of the samples is better than 10%, whereas the accuracy of the ICP-MS measurements is within 0.5–3.9% from replicate analyses of standard material BIR-1 and W-2a. All analyses were conducted at the Activation Laboratories of Ontario, Canada. Thin sections for petrographic studies were prepared in the Geology Department of Rhodes University, South Africa.

Results

Petrography

Examination of the 13 TNGB intrusive rock specimens and thin sections grouped the samples into mafic and intermediate based on their mineralogical composition, textures and geological settings. The mafic samples comprise gabbro, dolerite and feldspar porphyry from Twangiza and Namoya sites. The intermediate rocks include diorite and quartz diorite from Kamituga, Lugushwa and Namoya sites.

Feldspar porphyry

Under the microscope, this unit comprises plagioclase phenocrysts of up to 1–2 mm long and minor biotite widely distributed. The plagioclases display surficial alteration into sericite (Figure 3a). The groundmass comprises secondary minerals, including fine-grained sericite, calcite, epidote, quartz

and chlorite. Opaque minerals are arsenopyrite and pyrite.

Gabbro

Primary minerals include clinopyroxene, plagioclase and subordinate olivine. Secondary minerals for this unit are chlorite, epidote, sericite, carbonates and opaques (Figure 3d).

Dolerite

Mineralogical compositions for this unit include clinopyroxene, amphibole, orthoclase, plagioclase and biotite with feldspar oikocrysts (Figure 3e). The clinopyroxene is significantly altered and pseudomorphosed by hornblende which is altered into chlorite and carbonates.

Quartz diorite

Typical mineralogy shows phenocrysts of plagioclase, quartz, biotite and hornblende. Alteration of hornblende and plagioclase in their edges is typical into fine-grained secondary phases.

Diorite

Under the microscope, the samples display sub-porphyritic to equigranular texture, characterised by hornblende alteration, plagioclase, quartz, biotite and interstitial fine-grained plagioclase matrix (Figure 3f). Subordinate phases are chlorite, epidote, sericite and carbonate minerals, calcite and dolomite.

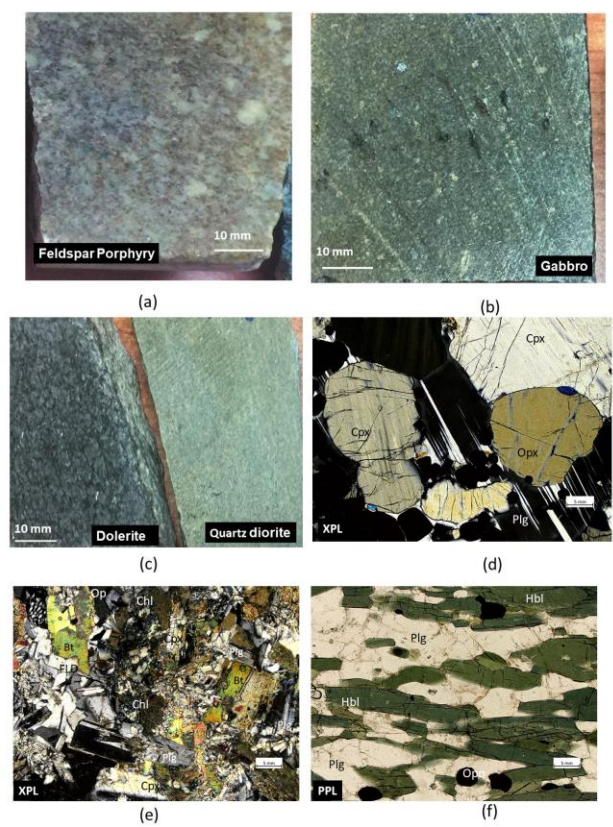


Figure 3: Photographs of TNGB igneous intrusive samples (a) a feldspar porphyry and (b), (c) dolerite and quartz-diorite specimen from Namoya, (d) a photomicrograph of gabbro showing pyroxene and plagioclase crystals, (e) a thin section of a dolerite sample from Namoya showing primary plagioclase, biotite, and alteration phases sericite, chlorite and carbonates, (f) a thin section of a diorite sample from Kamituga consisting hornblende, feldspar and opaque phase. Plg = plagioclase, Cpx = Clinopyroxene, Opx = Orthopyroxene, Bt = biotite, FLD = Feldspar, Hbl = hornblende, Chl = chlorite, Ep = epidote, Cb = carbonates and Op = opaque. PPL = plane polarised light, XPL = cross polarised light.

Geochemistry

Whole-rock geochemical data including trace element ratios for the 13 TNGB intrusive samples are presented in Table 1. All major element oxides are reported in weight per cent (wt.%) and trace elements are in parts per million (ppm). The concentrations of SiO₂ are within mafic and intermediate rock compositions as follows: gabbro = 46.77–48.39 wt.%, dolerite = 47.21 wt.%, feldspar porphyry = 48.50–53.21 wt.%, diorite = 52.24–55.36 wt.% and quartz diorite = 66.16 wt.%, consistent with the

petrographic examination estimated mineralogical compositions.

Element mobility

A key concern in studying geochemical characteristics of igneous rocks is elemental mobility that can be associated with the effects of hydrothermal alterations (Best 2002, Polat and Hoffmann 2003). Geochemical characteristics of igneous rocks, such as those from TNGB, can provide essential constraints on the origin, petrogenesis and ancient tectonic

environments of their emplacement (e.g. Pearce and Peate 1995, Polat and Hoffmann 2003). We adopted the approach proposed by Polat and Hoffmann (2003) of plotting mobile large ion lithophile elements (LILE) and immobile high field strength elements (HFSE) against immobile Zr to test the mobility of elements. The plots of LILE against Zr of the least altered samples have coefficients of correlation (R^2) between 0.5 to 0.75. In contrast, the other altered samples showed poor correlation coefficients with R^2 values below 0.5, except for Ba ($R^2 = 0.72$). Coefficient of correlation the all samples for HFSE and REE when plotted against Zr have

the following values: Th = 0.68–0.75, Nb = 0.84–0.98, Yb = 0.45–0.65, Gd = 0.78–0.95, Ta = 0.75–0.97, Y = 0.65, Hf = 0.96 and Lu = 0.61.

The correlation coefficients of greater than 0.75 suggest that the HFSE and REE remained immobile during the post-magmatic alteration events, and thus suitable for geochemical deduction of petrogenesis and tectonic settings. The Zr concentration plots against trace elements Nd, Nb, Gd and Ba classified the least altered and variably altered intrusive samples as Suites-1 and 2, respectively (Figure 4).

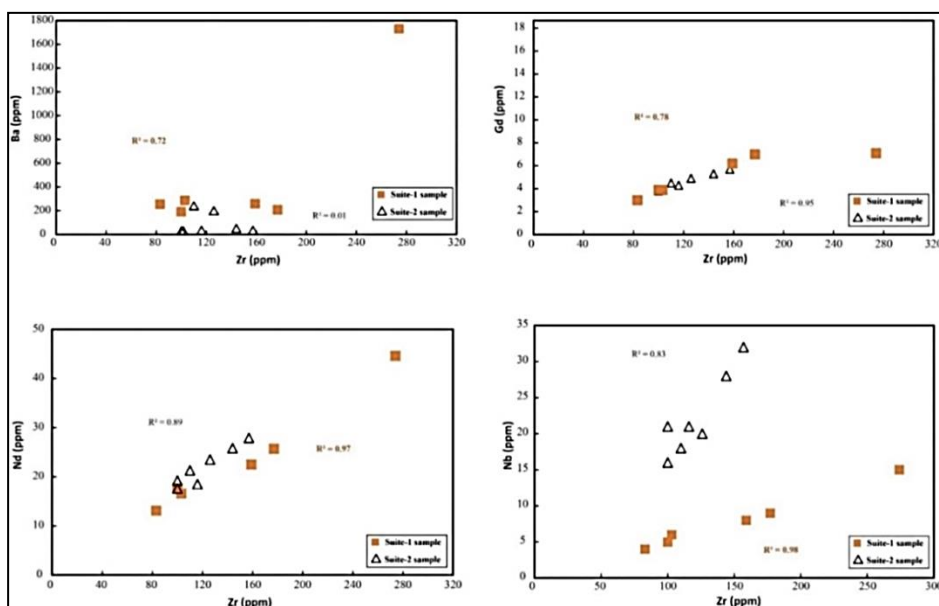


Figure 4: Bivariate plots of zirconium concentration (Zr) against selected HFSE, REE and LILE for TNGB igneous samples, top left) Zr vs Ba, top right) Zr vs Gd, bottom left) Zr vs Nd, and bottom right) Zr vs Nb. Samples are split into the least altered (Suite -1) and the variably altered (Suite-2) and their corresponding squared coefficient of correlation (R^2) values.

Classification

The samples were classified using the diagram of Nb/Y versus Zr/Ti adopted from by Pearce (1996) into two main groups: Sub-alkaline and andesitic basalts; and alkaline basalts (Figure 5a). Sub-alkaline basalts have higher Zr contents, lower Nb and correspond to the Kamituga and Lugushwa diorites. The andesitic basalt sample corresponds to the

quartz diorite sample (NM-INT-05). Samples clustering in the alkaline basalt field comprise gabbro, feldspar porphyry and dolerite from the Twangiza and Namoya sites. These sub-alkaline and andesitic basalt samples are classified as Suite-1 with LOI < 5 wt.% and include diorite and quartz diorite samples (Figure 5b).

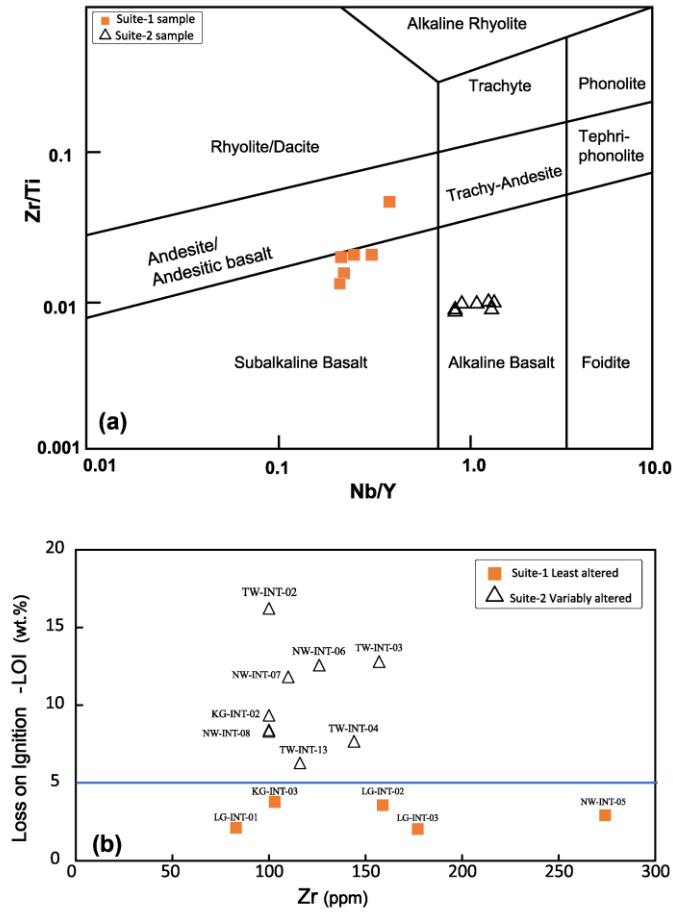


Figure 5: (a) A plot of immobile trace elements ratio Nb/Y versus Zr/Ti after Pearce (1996) classifying Suite-1 and Suite-2 rocks into sub-alkaline and andesitic basalts and alkaline basalts compositions respectively, (b) plots of Zr concentration against the loss on ignition content (LOI). The alkaline basalt samples include gabbro, dolerite and feldspar porphyry, classified as Suite-2 (Figure 5b).

Table 1: Major oxide and trace element abundances of mafic samples from the TNGB. Major oxide concentrations are given in weight per cent (wt.%), while trace elements abundances are reported in parts per million (ppm).

	Detection Limit	TW-INT-02	TW-INT-04	TW-INT-13	NM-INT-06	NM-INT-07	NM-INT-08	NM-INT-05	LG-INT-01	LG-INT-02	LG-INT-03	KG-INT-02	KG-INT-03	
SiO ₂	0.01	39.11	42.21	49.14	45.36	42.37	42.81	43.24	64.21	52.05	50.35	51.38	49.79	53.27
Al ₂ O ₃	0.01	11.7	14.1	17.26	13.21	13.62	14.56	15.43	15.42	13.12	13.07	13.04	12.1	13.1
Fe ₂ O _{3(T)}	0.01	8.16	7.86	9.32	16.94	12.04	12.12	11.31	6.57	9.55	15.71	15.76	10.07	11.08
MnO	0.001	0.11	0.1	0.06	0.11	0.19	0.15	0.15	0.08	0.16	0.26	0.24	0.17	0.2
MgO	0.01	8.56	7.64	6.35	9.96	6.34	7.11	8.97	2.11	8.65	4.7	4.76	5.67	6.9
CaO	0.01	9.69	6.67	0.76	3.19	6.46	5.88	8.67	0.73	9.84	5.84	7.52	8.14	7.43
Na ₂ O	0.01	3.88	6.06	6.96	3.42	2.81	3.19	1.85	3.27	1.7	1.22	2.02	1.2	0.49
K ₂ O	0.01	0.03	0.09	0.37	0.04	0.68	0.43	0.05	3.34	0.72	2.09	0.76	1.67	3.01
TiO ₂	0.001	1.44	2.41	2.21	1.89	2.04	1.82	1.59	0.97	0.67	1.78	1.93	0.75	0.79
P ₂ O ₅	0.01	0.19	0.3	0.29	0.24	0.35	0.32	0.26	0.13	0.09	0.21	0.24	0.09	0.1
LOI		16.23	12.81	7.68	6.29	12.58	11.93	8.41	2.92	2.11	3.57	2.03	9.35	3.78
Total		99.1	100.3	100.4	100.7	99.49	100.3	99.94	99.75	98.67	98.81	99.68	98.99	100.2
Mg#		65	63	55	51	51	59	50	48	53	36	62	35	35
Ti		10322	16561	14345	12084	13998	12382	10406	5990	4104	11070	11807	4964	4921
Sc	1	26.00	28.00	32.00	39.00	29.00	25.00	22.00	17.00	34.00	36.00	39.00	28.00	32.00
Be	1	1.00	1.00	1.00	1.00	1.00	bdl	bdl	2.00	bdl	1.00	1.00	2.00	1.00
V	5	199.00	313.00	339.00	270.00	240.00	210.00	184.00	97.00	201.00	373.00	407.00	221.00	241.00
Cr	20	490.00	190.00	270.00	540.00	110.00	100.00	100.00	90.00	370.00	100.00	100.00	230.00	320.00
Co	1	63.00	28.00	30.00	64.00	52.00	47.00	63.00	19.00	46.00	45.00	48.00	40.00	42.00
Ni	20	220.00	60.00	70.00	230.00	70.00	120.00	220.00	20.00	160.00	60.00	40.00	60.00	70.00
Rb	2	bdl	8.00	14.00	2.00	32.00	23.00	bdl	136.00	33.00	116.00	29.00	297.00	268.00
Sr	2	55.00	27.00	125.00	105.00	204.00	324.00	317.00	153.00	183.00	180.00	127.00	84.00	96.00
Y	2	15.00	23.00	21.00	18.00	22.00	20.00	16.00	36.00	17.00	36.00	39.00	19.00	18.00
Zr	4	100.00	157.00	144.00	116.00	126.00	110.00	100.00	274.00	83.00	159.00	177.00	100.00	103.00
Nb	1	21.00	32.00	28.00	21.00	20.00	18.00	16.00	15.00	4.00	8.00	9.00	5.00	6.00
Cs	0.5	bdl	0.90	bdl	bdl	2.40	1.90	bdl	11.60	2.60	27.90	2.90	287.00	137.00
Ba	3	23.00	30.00	47.00	31.00	197.00	237.00	29.00	1732.00	255.00	259.00	208.00	191.00	286.00
La	0.1	18.80	26.70	24.60	16.60	19.90	17.80	15.00	49.80	12.80	19.50	22.30	18.90	16.80
Ce	0.1	38.30	56.30	51.20	35.50	43.30	38.80	32.50	103.00	27.50	43.30	47.30	38.00	35.40
Pr	0.05	4.58	6.74	6.25	4.37	5.50	5.00	4.17	11.80	3.25	5.30	6.01	4.36	4.09

Nd	0.1	19.20	27.90	25.80	18.50	23.50	21.30	17.60	44.60	13.10	22.50	25.70	17.70	16.60
Sm	0.1	4.20	6.00	5.80	4.30	5.20	4.70	4.00	8.60	3.00	5.60	6.60	4.10	3.90
Eu	0.05	0.90	1.34	1.75	1.87	1.52	1.83	1.52	1.74	0.88	1.65	1.84	1.11	1.03
Gd	0.1	3.80	5.70	5.30	4.30	4.90	4.50	3.80	7.10	3.00	6.20	7.00	3.90	3.90
Tb	0.1	0.60	0.90	0.80	0.70	0.80	0.70	0.60	1.10	0.50	1.10	1.20	0.70	0.70
Dy	0.1	3.30	4.90	4.50	4.10	4.60	4.40	3.50	6.80	3.20	6.90	7.60	4.30	4.10
Ho	0.1	0.60	0.90	0.80	0.70	0.90	0.80	0.70	1.40	0.70	1.40	1.50	0.80	0.80
Er	0.1	1.80	2.60	2.20	2.00	2.40	2.30	1.90	4.00	2.00	4.10	4.50	2.40	2.40
Tm	0.05	0.24	0.37	0.29	0.28	0.35	0.33	0.27	0.59	0.29	0.58	0.68	0.35	0.34
Yb	0.1	1.50	2.20	1.80	1.70	2.20	2.00	1.60	4.00	1.90	3.90	4.40	2.30	2.20
Lu	0.04	0.21	0.31	0.28	0.26	0.33	0.29	0.24	0.59	0.29	0.61	0.66	0.33	0.34
Hf	0.2	2.50	3.60	3.20	2.70	2.80	2.50	2.40	6.50	2.40	4.60	4.40	2.50	2.60
Ta	0.1	1.50	2.20	1.90	1.50	1.30	1.20	1.00	1.20	0.30	0.60	0.70	0.40	0.50
Tl	0.1	0.20	bdl	bdl	bdl	0.20	0.20	bdl	0.60	bdl	0.20	0.20	1.90	1.60
Pb	5	bdl	bdl	bdl	bdl	bdl	bdl	9.00	16.00	6.00	11.00	9.00	9.00	10.00
Th	0.1	1.90	2.80	2.30	1.80	1.60	1.10	1.00	14.10	3.60	5.20	5.20	5.80	5.70
U	0.1	0.50	0.70	0.80	0.40	0.40	0.30	0.20	3.40	0.70	1.10	1.10	1.10	1.20
Ti/Zr		103.23	105.49	99.62	104.18	111.10	112.57	104.07	21.86	49.45	69.62	66.72	49.65	47.78
Nb/Ta		14.00	14.55	14.74	14.00	15.38	15.00	16.00	12.50	13.33	13.33	12.86	12.50	12.00
Nb/Th		11.05	11.43	12.17	11.67	12.50	16.36	16.00	1.06	1.11	1.54	1.73	0.86	1.05
Ce/Pb		nd	nd	nd	nd	nd	nd	3.61	6.44	4.58	3.94	5.26	4.22	3.54
La/Nb		0.90	0.83	0.88	0.79	1.00	0.99	0.94	3.32	3.20	2.44	2.48	3.78	2.80
Zr/Hf		40.00	43.61	45.00	42.96	45.00	44.00	41.67	42.15	34.58	34.57	40.23	40.00	39.62
Th/Ta		1.27	1.27	1.21	1.20	1.23	0.92	1.00	11.75	12.00	8.67	7.43	14.50	11.40
Th/Yb		1.27	1.27	1.28	1.06	0.73	0.55	0.63	3.53	1.89	1.33	1.18	2.52	2.59
Th/La		0.10	0.10	0.09	0.11	0.08	0.06	0.07	0.28	0.28	0.27	0.23	0.31	0.34
Nb/Yb		14.00	14.55	15.56	12.35	9.09	9.00	10.00	3.75	2.11	2.05	2.05	2.17	2.73
Zr/Y		6.67	6.83	6.86	6.44	5.73	5.50	6.25	7.61	4.88	4.42	4.54	5.26	5.72
Ta/Yb		1.00	1.00	1.06	0.88	0.59	0.60	0.63	0.30	0.16	0.15	0.16	0.17	0.23
La/Ta		12.53	12.14	12.95	11.07	15.31	14.83	15.00	41.50	42.67	32.50	31.86	47.25	33.60
Eu/Eu*		0.69	0.70	0.96	1.33	0.92	1.22	1.19	0.68	0.90	0.86	0.83	0.85	0.81
(La/Yb)CN		8.99	8.71	9.80	7.00	6.49	6.38	6.72	8.93	4.83	3.59	3.64	5.89	5.48

Trace elements geochemistry

Trace elements and ratios are essential in characterising rock units and highlighting the various subtle changes in alteration-prone zones (Rollinson 1993). They are applied for the TNGB intrusive rocks to distinguish the samples. Suite-1 rocks have trace element ratios $Ti/Zr = 22-70$ which is below the chondritic ratio $Ti/Zr = 116$ of Sun and McDonough (1989). Ratios of Nb/Ta (12.00–13.33) for Suite-1 fall below the typical mid-oceanic-ridge basalts (MORB) and oceanic island basalts (OIB; i.e., $Nb/Ta = 15-16$), indicating crustal inputs and contamination of the magma source (Green 1995). Comparatively, Suite-1 samples have Zr/Hf ratios of between 35–42 that are within the chondritic value of 36 as reported in Sun and McDonough (1989). However, their La/Nb ratios that are between 2.4–3.8 indicate typical arc generated magmas that assimilated continental crust material (see Stern 2002).

Suite-2 samples have ratio of $Ti/Zr = 100-113$; this feature is comparable to the chondritic Ti/Zr ratio of 116, while Zr/Hf value of 45 is above the corresponding chondritic value (i.e. Sun and McDonough 1989). The obtained ratios Nb/Ta of 14.00–16.00 for Suite-2 rocks are within the mantle and chondrite material value of $Nb/Ta = \sim 17.5$ (Sun and McDonough 1989). Furthermore, Suite-2 rocks have $La/Nb = 0.8-1.0$ that are below the threshold ratio of

1.4, suggesting an oceanic plateau basalts affinity (Condie 1984, Floyd 1989, Rudnick 1995).

The primitive mantle-normalised trace element diagrams for the two Suites have contrasting characteristics. Suite-1 has positive anomalies of LILE (Cs, Rb, K and Pb) and negative Nb, Ta, and Ti anomalies (Figure 6a). The chondrite-normalised ratios $(La/Yb)_{CN}$ (3.59–8.93) and negative Eu^* anomalies ranging between 0.7–0.9 for Suite-1 samples suggest significant plagioclase fractionation from their melts. Suite-1 rocks are also characterised by relatively flat REE patterns in the chondrite-normalised diagram, indicating light REE enrichments as compared to the middle and heavy REE (Figure 6b).

In contrast, Suite-2 shows relative enrichments in Cs and Pb, negative anomalies of Rb, K, Sr, and average values of Nb, Ta, and Ti in the primitive mantle normalised diagram (Figure 6a). The chondrite normalised REE patterns of Suite-2 samples are generally flat with relatively higher chondrite-normalised ratios $(La/Yb)_{CN}$ of 6.4–9.8 and negative to positive anomalies of Eu anomalies ($Eu^* = 0.7-1.3$). These Suite-2 rocks have distinct REE characteristics and are more REE fractionated than rocks of Suite-1 (Figure 6b).

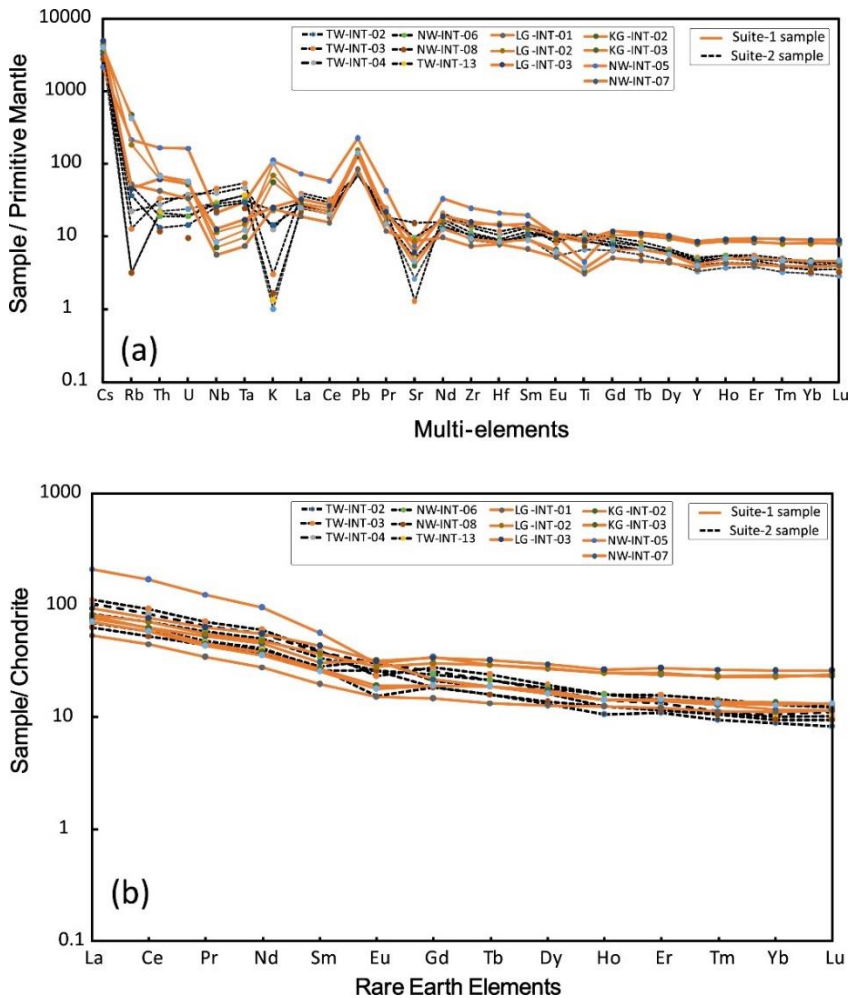


Figure 6: Trace elements and REE diagrams of the igneous rocks (Suite-1 and Suite-2). (a) multiple elements normalised to primitive mantle values and (b) REE concentrations normalised to chondritic values. Normalising values are after Sun and McDonough (1989).

Discussions

Tectonic settings

The negative Nb-Ta and Ti anomalies with positive LILE anomalies and flat REE in the primitive mantle-normalised trace elements diagram characterise Suite-1 samples (Figure 6a). The negative Nb, Ta and Ti with positive LILE anomalies is a typical arc magmatism feature and crustal material contamination of mantle-derived magmas (Best 2002). The origin of negative Nb, Ta and Ti anomalies in these arc rocks can be attributable to the relative preferential mobilisation of LILE by hot fluids under

pressure, leading to their enrichment over the HFSE in a subduction wedge environment (Green 1995, Pearce 1996).

Alternative explanations point to a refractory phase such as rutile, which HFSE are highly compatible, been retained in the mantle magmatic source zone (Gao et al. 2007) or, the HFSE are sequestered into residual hornblende resulting in the negative anomalies (Defant and Drummond 1990, Gao et al. 2007). In some other cases, Back Arc Basin Basalts (BABB) have similar trace element patterns of negative Nb, Ta and Ti anomalies with enrichments of LREE and

composition transitional between ocean-floor and island arc magmas (Stern 2002). Nevertheless, these back-arc basin basalts lack contamination by upper crustal material due to their rapid emplacement through thin crustal oceanic rift regions. Suite-2 rocks are characterised by neutral to positive anomalies of HFSE (Nb, Ta), positive anomalies of Cs, Pb and notable negative Rb, Th and Sr relative to REE (Figure 6a). These features with exceptional highly mobile LILE are typical of within plate basalts (Pearce and Peate 1995).

Suite-1 samples cluster in the active continental arc field in the discrimination diagram (Figure 7a) of Yb against Th/Ta after Gorton and Schandl (2000), revealing the relative enrichment of Th, due to crustal material input into mantle generated magma source (Pearce and Peate 1995). In the Ta/Yb against Th/Yb diagram (Figure 7b, Pearce 1989), Suite-1 samples align in the active continental margin.

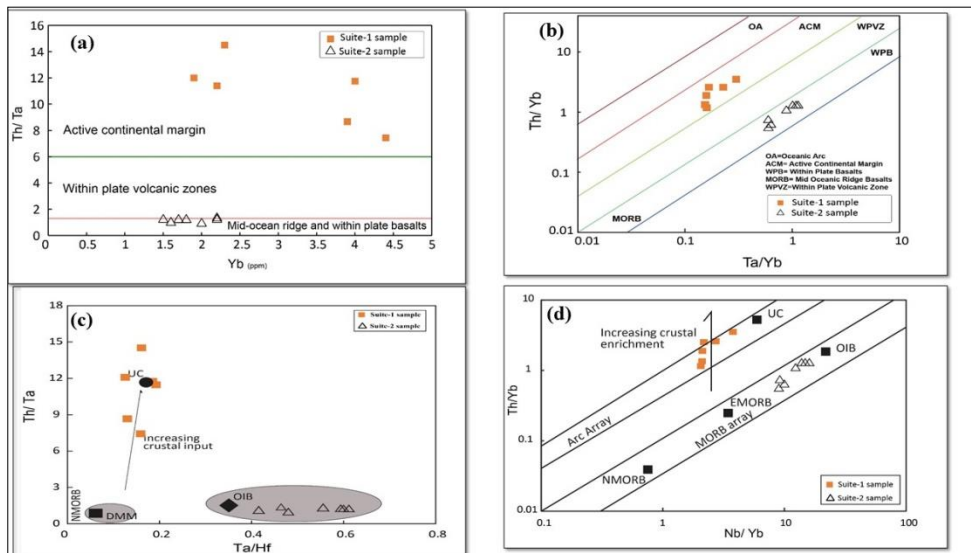


Figure 7: Trace elements ratio diagrams for the TNGB igneous intrusive rock samples. (a) Yb against Th/Ta diagram after Gorton and Schandl (2000), (b) Ta/Yb versus Th/Yb diagram after Pearce (1983), (c) diagram of Ta/Hf versus Th/Ta after Manya (2016), and (d) diagram of Nb/Yb against Th/Yb after Pearce and Peate (1995). N-MORB, EMORB and OIB are from Sun and McDonough (1989), UC from Rudnick and Gao (2003) and DMM data from Workman and Hart (2005).

Suite-2 samples plot between the enriched MORB and OIB (Oceanic Island Basalt) fields in the Yb against Th/Ta diagram (Figure 7a). The diagram suggests and collaborates with the absence of any crustal material contamination in the petrogenesis of Suite-2 rocks (Pearce and Peate 1995, Sun and McDonough 1995, Best 2002). In the Ta/Yb against Th/Yb diagram (Figure 7b, Pearce 1983), Suite-2 samples plot in the within plate basalts array to transitional

MORB- EMORB fields. These Suite-2 rocks have trace element characteristics resembling oceanic plateau basalt intrusions, characterised by rapid submarine sheet flow extrusion, depletions in REE chondrite-normalised patterns relative to NMORB coupled with positive anomalies of Nb, Ta and Ti (Floyd 1989).

Petrogenesis

The immobile trace element ratios Zr/Hf and Ti/Zr of TNGB samples (Table 1) indicate that they are mantle-derived magmas. The lower values of Ti/Zr ratios than typical chondrite values suggest crustal material assimilation that lowered the balance by increasing Zr contents for Suite-1 rocks (e.g. Pearce and Peate 1995). Suite-2 rocks have Ti/Zr = 100–113 (mean =106) within the chondritic ratio of Ti/Zr = 116, indicating a mantle source with a composition between an enriched MORB and OIB (Pearce 1996).

The trace element ratios Nb/Th can distinguish melts affected by arc generated fluids (Green 2006). Rocks affected by arc-generated fluids have Nb/Th < 5 while those not affected have Nb/Th > 7 (Green 2006). Suite-1 samples have Nb/Th = 1–2, a feature suggestive that they were affected by arc-generated fluids. In contrast, Suite-2 rocks have Nb/Th = 11–16, which precludes the participation of arc-generated fluids in their genesis (Green 2006).

Suite-1 rocks plot near the upper crust field in the Ta/Hf vs Th/Ta diagram (Figure 7c), this feature suggests crustal contamination of the protolith (Manya 2016, Figure 7c). In the same diagram, Suite-2 rocks plot in the Oceanic Islands Basalts (OIB) field indicating a mantle generated source with EMORB-like composition and no crustal material contamination for the protolith (see Manya 2016, Figure 7c). The Nb/Yb versus Th/Yb plot (Figure 7d) after Pearce and Peate (1995) plots Suite-1 rocks in the field overlapping continental and oceanic arc fields, suggesting a combination of subduction enrichment and continental crust assimilation. On the other hand, Suite-2 rocks align along the MORB-IOB field, suggesting partial melting and fractional crystallisation dominated processes, with no contamination with crustal material (Figure 7d, Pearce and Peate 1995).

Conclusions

Geochemical results for samples collected from the Twangiza-Namoya Gold Belt suggest the following:

- (i) Intrusive igneous rocks from the TNGB comprise two geochemically and petrographically distinct rock suites; Suite-1 rocks from the Lugushwa, Kamituga and Namoya sites have sub-alkaline and andesitic basalt composition. Suite-2 rocks from the Twangiza and Namoya sites have alkaline basalt composition.
- (ii) Suite-1 rocks trace element ratios La/Nb, Zr/Hf and Ti/Zr typical are of arc magmas. Primitive normalised Nb, Ta, Ti anomalies and relative LILE enrichments in primitive mantle normalised diagram suggest an active continental margin setting for Suite-1. Suite-2 rocks have ratios of La/Nb < 1 that are akin to oceanic plateau basalts. Additionally, chondritic Ti/Zr and Zr/Hf ratios, negative Rb, K, Sr anomalies in tandem with neutral to positive Nb, Ta, Pb, Ti anomalies in the primitive mantle-normalised diagram suggest a within plate basalts setting.
- (iii) Both suites display typical near-flat REE chondrite-normalised patterns showing LREE fractionations relative to HREE and slightly negative to positive Eu anomalies, features that are typical to moderate plagioclase fractionation from the mantle-derived melts with minor REE fractionation.
- (iv) Insights from trace elemental ratio diagrams of Ta/Hf vs Th/Ta combined with Nb/Yb vs Th/Yb insights suggest that the source of Suite-1 rocks were from depleted mantle-derived NMORB magmas affected by metasomatisation and upper crust material contamination. Insights from elemental diagrams of Ta/Hf vs Th/Ta and Nb/Yb vs Th/Yb indicate that Suite-2 rocks originated from mantle-derived source with composition between EMORB and IOB.

Acknowledgements

We would like to thank the Chief Editor, Prof. John A.M. Mahugija, and the three anonymous reviewers whose critical reviews significantly improved the output of this manuscript. The second author (CHK)

dedicates this article to the late Maarten de Wit, one of dedicated extraordinary lovers of nature and of the geology of Africa. Maarten had an unrivalled memory of thousands of outcrops he visited across Africa including the DRC.

Conflict of Interest: No conflict of interest.

References

- Best MG 2002 *Igneous and Metamorphic Petrology*, Second edition, *Blackwell Sci. Ltd.*, 717p.
- Condie KC 1984 Secular variation in the composition of basalts: an index to mantle evolution. *J. Petrol.* 26(3): 545-563.
- Debruyne D, Hulsbosch N, Van Wilderode J, Balcaen, L, Vanhaecke F and Muchez P 2015 Regional geodynamic context for the Mesoproterozoic Kibara belt (KIB) and the Karagwe-Ankole Belt: Evidence from geochemistry and isotope in the KIB. *Precamb. Res.* 24: 82-97.
- Defant MJ and Drummond MS 1990 Derivation of some modern arc magmas by melting of young subducted lithosphere. *Nat.* 347: 622-665.
- Fernandez-Alonso M, Cutten H, De Waele B, Tack L, Tahon A, Baudet D and Barritt SD 2012 The Mesoproterozoic Karagwe-Ankolean Belt (Formerly the NE Kibara Belt): the result of prolonged extensional intracratonic basin development punctuated by two short-lived far-field compressional events. *Precamb. Res.* 216-219: 63-86.
- Floyd PA 1989 Geochemical features of intraplate oceanic plateau basalts. *Geol. Soc. Lond. Spec. Publ.* 42: 215-230.
- Gao J, John T, Klemd R and Xiong XM 2007 Mobilisation of Ti-Nb-Ta during subduction: evidence from rutile bearing dehydration segregation and veins hosted in eclogite, Tianshan, NW China. *Geochim. Cosmochim. Acta.* 71: 4974-4996.
- Green TH 1995 Significance of Nb-Ta as an indicator of geochemical processes in the crust-mantle system. *Chem. Geol.* 120(3-4): 347-359.
- Green NL 2006 Influence of slab thermal structure on basalt source regions and melting condition: REE and HSE constraints from the Garibaldi volcanic belt, northern Cascadia subduction system. *Lithos.* 87: 23-49.
- Gorton MP and Schandl ES 2000 From Continents to Island arcs: A geochemical index of tectonic setting for Arc-related and Within-plate felsic to intermediate volcanic rocks. *Canad. Mineral.* 38: 1065-1073.
- Hanson RE 2003 Proterozoic geochronology and tectonic evolution of Southern Africa. *Geol. Soc. Lond. Spec. Publ.* 206: 427-463.
- Jenner GA 1996 Trace element geochemistry of igneous rocks: geochemical nomenclature and analytical geochemistry; In Wyman DA ed, Applications for Massive Sulphide Exploration. *GAC, Short Course Notes*, 12: 51-77.
- Klerkx J, Liegeois JP, Lavreau J and Claessens W 1987 Crustal evolution of the Northern Kibaran Belt, Eastern and Central Africa. In: A Kroner ed., Proterozoic Lithospheric Evolution. *Geodyn. Ser. AGU* 17: 217-233.
- Koegelenberg C and Kisters AFM 2014 Tectonic wedging, back-thrusting and basin development in the frontal parts of the Mesoproterozoic Karagwe-Ankole Belt in NW Tanzania. *J. Afri. Earth Sci.* 97: 87-89.
- Manya S 2016 Geochemistry of the mafic volcanic rocks of the Buzwagi gold mine in the Neoproterozoic Nzega greenstone belt, Northern Tanzania. *Lithos.* 264: 86-95.
- Milesi JP, Toteu SF, Deschamps Y, Feybesse JL, Lerouge C, Cocherie A, Penaye J, Tchameni R, Moloto-A-Kenguemba G, Kampunzu HAB, Nicol N, Duguey E, Leistel JM, Saint-Martin M, Ralay F, Henry C, Bouchot V, Doumngang JC and Cailteux J 2006 An overview of the geology and major ore deposits of Central Africa: Explanatory note for the 1:4,000,000 map "Geology and Major Ore deposits of Central Africa", *J. Afri. Earth Sci.* 44(4-5): 571-595.

- Olesik JW 1991 Elemental analysis using ICP-OES and ICP-MS. *Anal. Chem.* 63(1): 12A-21A.
- Pearce JA 1983 Role of the sub-continental lithosphere in magma genesis at active continental margins. In: Hawkesworth CJ and Norry MJ (Eds), *Continental Basalts and Mantle Xenoliths. Shiva Publ.* 230-249.
- Pearce JA and Peate DW 1995 Tectonic implications of the composition of volcanic arc magmas. *Annu. Rev. Earth Planet. Sci.* 23: 251-285.
- Pearce JA 1996 A user's guide to basalt discrimination diagrams. In: Wyman DA (Ed), *Trace Element Geochemistry of Volcanic Rocks: Application for Massive Sulphide Exploration, GAC, Short Course Notes* 12: 79-113.
- Pohl WL, Biryabarema M and Lehmann B 2013 Early Neoproterozoic rare metal (Sn, T, W) and gold metallogeny of the Central Africa Region: a review. *Appl. Earth Sci.* 122: 66-82.
- Polat A and Hoffmann AW 2003 Alteration and geochemical patterns in the 3.7-3.8 Ga Isua greenstone belt, West Greenland. *Precamb. Res.* 126: 197-218.
- Rollinson HR 1993 *Using Geochemical Data: evaluation, presentation, interpretation.* Longman Group UK, 352 p.
- Rudnick RL 1995 Making the continental crust. *Nat.* 378: 573-578.
- Rudnick RL and Gao S 2003 Composition of the continental crust. In: Rudnick RL (Ed), *The crust, Holland, H.D., Turekian, K.K (Eds.), Treat. Geochem.* 3: 1-64 p.
- Stern RJ 2002 Subduction zones. *Rev. Geophys.* 40(4): 1012.
- Sun SS and McDonough WF 1989 Chemical and isotopic systematics of oceanic basalts: implication for mantle composition and processes. In: Saunders AD and Norry MJ (Eds.), *Magmatism in the Ocean Basins. Geol. Soc. Lond. Spec. Publ.* 42: 313-345.
- Sun SS and McDonough WF 1995 The composition of the Earth. *Chem. Geol.* 120: 223-253.
- Tack L, Wingate MTD, De Waele B, Meert J, Belousova E, Griffin B, Tahon A and Fernandez-Alonso M 2010 The 1375 Ma Kibaran event in Central Africa: prominent emplacement of bimodal magmatism under extensional regime. *Precamb. Res.* 180: 63-84.
- Walembe KMA 2001 *Geology, Geochemistry and Tectono-Metallogenic evolution of Neoproterozoic Gold deposits in the Kadubu area, Kivu, Democratic Republic of Congo.* PhD Thesis. Johannesburg, South Africa. University of Witwatersrand. 491 p.
- Walembe KMA and Master S 2005 Neoproterozoic diamictites from the Itombwe synclinorium, Kivu Province, Democratic Republic of Congo: paleoclimatic significance and regional correlations. *J. Afr. Earth Sci.* 42: 200-210.
- Workman RK and Hart SR 2005 Major and trace element composition of the depleted MORB mantle (DMM). *Earth Planet Sci. Lett.* 231: 53-72.